MODEL BASED BRAKING CONTROL WITH SUPPORT BY ACTIVE STEERING

Matthias Schorn * **Jürgen Schmitt** * **Ulrich Stählin** *
Rolf Isermann *

* *Institute of Automatic Control, TU Darmstadt*
Landgraf-Georg-Str. 4, 64283 Darmstadt, Germany
{MSchorn,JSchmitt,UStaehlin,RIsermann}@iat.tu-darmstadt.de

Abstract: Model based feedback control strategies for electrohydraulic braking and active steering systems in passenger cars are considered. Simulation results with a complex vehicle model and measurements from test drives with a real car are shown for brake control. For a μ-split road surface additional drive dynamics control is required like ESP or active front steering (AFS). Therefore, an AFS feedback controller is applied to stabilize the vehicle. Furthermore, the braking control is improved by AFS, assisting the driver to brake in critical situations.

Keywords: Braking Control, Driver Assistance, Stability Control, Electrohydraulic Brake, Vehicle Dynamics

1. INTRODUCTION

The development of driver assistance systems is intended to reduce the number of accidents and to improve comfortable driving. Examples for active assistance systems are antilock braking (ABS), the electronic stability program (ESP) and active front steering (AFS). A further development towards automatic driving also requires controlled braking. Therefore, a braking control system is designed by using an electrohydraulic brake (EHB), which is in production since 2003. However, controlled braking on μ-split leads to unstable behavior, if the driver doesn't countersteer. To automate this correction, AFS can be used. Therefore, a further steering control system is designed to compensate yaw motion automatically in case of braking.

2. BRAKING CONTROL

Developing a vehicle feedback control system, different steps have to be passed:

- Derivation of a simplified low-order model for controller design
- Controller optimization
- Analysis of closed loop stability
- Simulation with validated high-order (complex) model
- Test of the controller with the real system

2.1 Design of the braking controller

For the force transmission between tire and road surface, with the assumption of a straight run, it holds:

$$F_{\mathrm{L}}(t) = \mu \cdot F_{\mathrm{z}}(t) \tag{1}$$

The wheel dynamics are described by

$$J_{\mathrm{W}}\dot{\omega}(t) = T_{\mathrm{Dr}}(t) - T_{\mathrm{Br}}(t) - r_{\mathrm{dyn}}F_{\mathrm{L}}(t) \tag{2}$$

where T_{Dr} and T_{Br} are the drive and the brake torque, J_{W} is the moment of inertia of the wheel and r_{dyn} the dynamic tire radius. F_{L} is the longitudinal tire force, $\dot{\omega}$ the angular speed of the wheel. The longitudinal motion of the vehicle is described by

$$m \cdot \ddot{x}(t) = F_{\mathrm{L_{FL}}}(t) + F_{\mathrm{L_{FR}}}(t) + F_{\mathrm{L_{RL}}}(t) + F_{\mathrm{L_{RR}}}(t) + F_{\mathrm{disturbance}}(t) \quad (3)$$

where $F_{\mathrm{disturbance}}$ includes forces caused for example by wind and slope. Electrohydraulic braking systems (Robert Bosch GmbH, 2003) and (Breuer and Bill, 2003) allow to realize a feedback controlled braking system. The braking force for each wheel follows with $T_{\mathrm{Dr}} = 0$ and $J_{\mathrm{W}}\dot{\omega} << T_{\mathrm{Br}}$:

$$F_{\mathrm{L_{ii}}}(t) \cong -\frac{T_{\mathrm{Br_{ii}}}(t)}{r_{\mathrm{dyn}}} \quad (4)$$

Introducing $T_{\mathrm{B}} = T_{\mathrm{Br_{FL}}} + T_{\mathrm{Br_{FR}}} + T_{\mathrm{Br_{RL}}} + T_{\mathrm{Br_{RR}}}$ Eq. (3) leads to:

$$\ddot{x}(t) = -\frac{T_{\mathrm{B}}(t)}{m \cdot r_{\mathrm{dyn}}} + \frac{F_{\mathrm{disturbance}}(t)}{m} \quad (5)$$

The brake torque can be modeled as a second order system, assuming the same transfer behavior for all four wheel brakes, (Germann, 1997):

$$G_{\mathrm{EHB}}(s) = \frac{T_{\mathrm{B}}(s)}{p_{\mathrm{B}}(s)} = \frac{K_{\mathrm{EHB}}}{1 + 2\frac{D_{\mathrm{EHB}}}{\omega_{0_{\mathrm{EHB}}}} \cdot s + \frac{1}{\omega^2_{0_{\mathrm{EHB}}}} \cdot s^2} \quad (6)$$

K_{EHB}, $\omega_{0_{\mathrm{EHB}}}$ and D_{EHB} contain the parameters of the brake (Reimpell and Burckhardt, 1991) and the force distribution between front and rear axle. Introducing Eq. (5) with $F_{\mathrm{disturbance}} = 0$ leads to the transfer function of vehicle braking:

$$G_{\mathrm{B}}(s) = \frac{\ddot{x}(s)}{p_{\mathrm{B}}(s)} = \frac{-\frac{K_{\mathrm{EHB}}}{m \cdot r_{\mathrm{dyn}}}}{1 + 2\frac{D_{\mathrm{EHB}}}{\omega_{0_{\mathrm{EHB}}}} \cdot s + \frac{1}{\omega^2_{0_{\mathrm{EHB}}}} \cdot s^2} \quad (7)$$

A linear PI-controller is used as braking controller:

$$G_{\mathrm{C}}(s) = \frac{p_{\mathrm{B}}(s)}{x_{\mathrm{d}}(s)} = K_{\mathrm{R}}\left(1 + \frac{1}{T_{\mathrm{I}} \cdot s}\right) \quad (8)$$

The control loop parameters are designed by pole placement.

2.2 Simulation results

A nonlinear two-track model has been developed and validated for a test vehicle VW Golf IV. This nonlinear two-track model is similar to models for other test vehicles (Halfmann and Holzmann, 2003). Actuators (e.g. for the active braking system and active front steering) have been integrated. This way, control strategies can be developed within a validated environment (Schmitt *et al.*, 2004*b*). The vehicle model has six degrees of freedom for pitch, roll, yaw and longitudinal, lateral and vertical motion. Fig. 1 shows the agreement of the used simulation model with measured data. The driving maneuver was a lane change at a velocity of about $10\,\frac{\mathrm{m}}{\mathrm{s}}$.

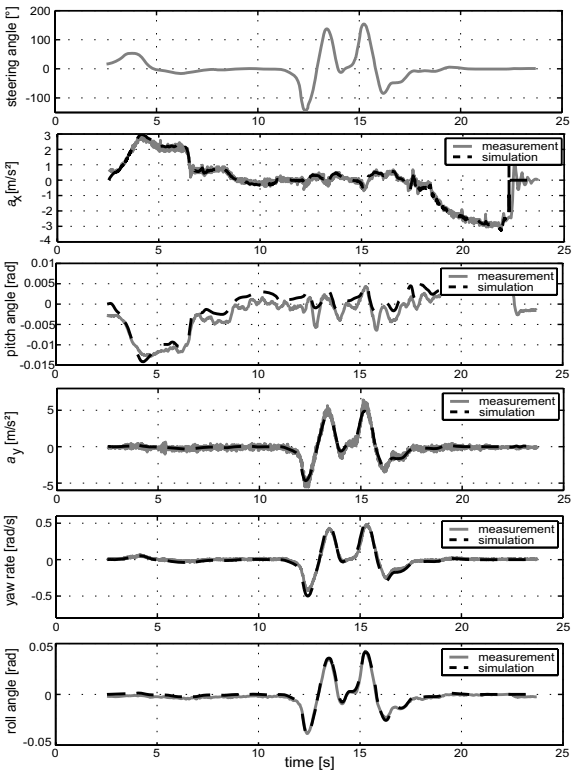

Fig. 1. Verification of the used two-track-model for a lane change

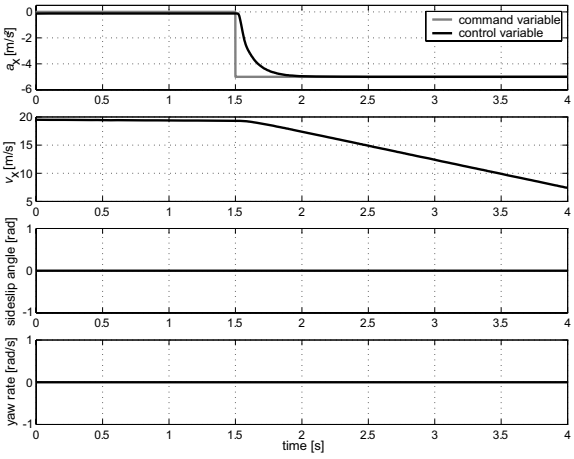

Fig. 2. Simulation results with $a_{\mathrm{x}} = -5\,\frac{\mathrm{m}}{\mathrm{s}^2}$ on homogenous surface (ABS not active)

In Fig. 2 a deceleration of $a_{\mathrm{x}} = -5\,\frac{\mathrm{m}}{\mathrm{s}^2}$ is shown, using the controller designed above and using the complex simulation model for the test vehicle VW Golf IV. The friction coefficient was homogenous at $\mu = 1$.

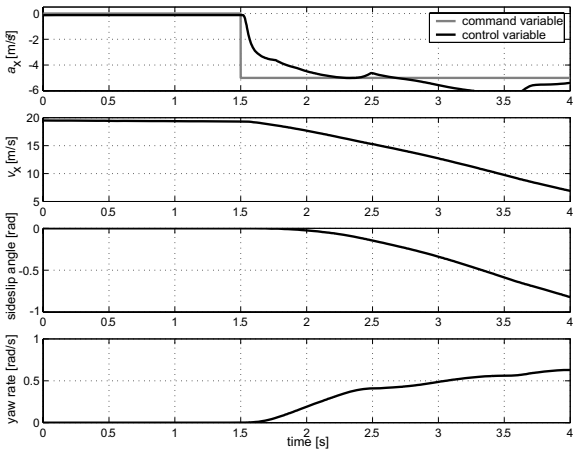

Fig. 3. Simulation results with $a_{\mathrm{x}} = -5\,\frac{\mathrm{m}}{\mathrm{s}^2}$ on μ-split surface (ABS not active)

As can be seen, the control input and the control variable behave as expected.

Another simulation maneuver, braking on a μ-split surface, is shown in Fig. 3. The vehicle gets unstable because of different tire forces at the wheels on μ-high and on μ-low surface which result in a yaw moment. Therefore, in addition to the brake control, driver assistance systems like antilock braking system (ABS), the electronic stability system (ESP) or active front steering (AFS) are required. To stabilize the vehicle on μ-split road surfaces, a feedback controller approach for an active front steering system is presented in section 3.

2.3 Experimental results for brake control

The test vehicle is equipped with an electrohydraulic brake. Many variables can be measured and recorded, e.g. the longitudinal, lateral and vertical acceleration of the center of gravity. Controllers can be designed in MATLAB/SIMULINK and, after using a target compiler, can be executed on a realtime hardware. In Fig. 4 the measured data of a test run are shown for brake control. The controlled deceleration follows precisely the setpoint.

The controller was tested in cornering maneuvers, too, showing good results. Control deviations occur because of disturbances in the real vehicle, e.g. noisy signals, and road unevenness.

3. ACTIVE FRONT STEERING CONTROL

The objective of an active front steering control system is to regulate the yaw rate $\dot{\psi}(t)$ in critical driving maneuvers. The control system (Fig. 5) is realized by a model reference controller which makes the vehicle follow the desired

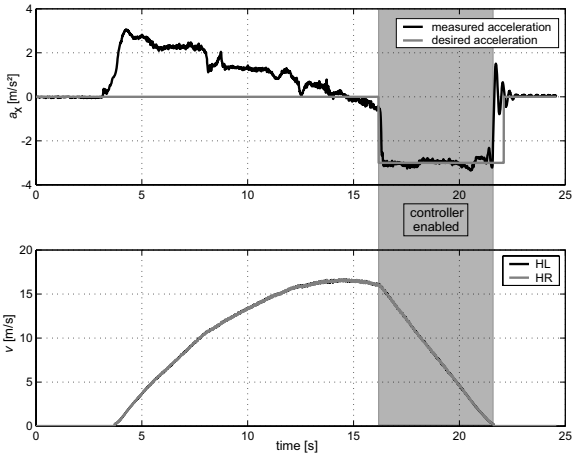

Fig. 4. Test results for controlled braking. Reference value: $a_{\mathrm{x}} = -3\,\frac{\mathrm{m}}{\mathrm{s}^2}$

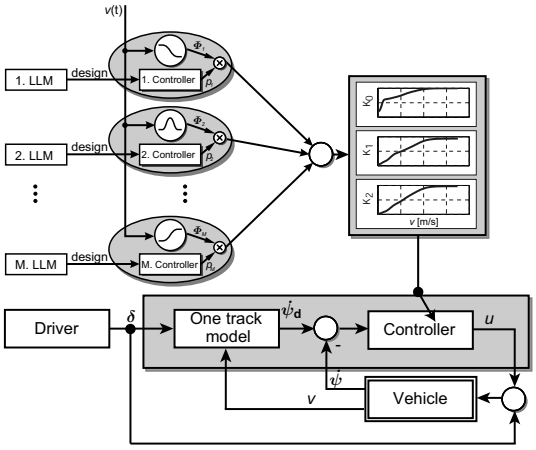

Fig. 5. Control concept for active steering

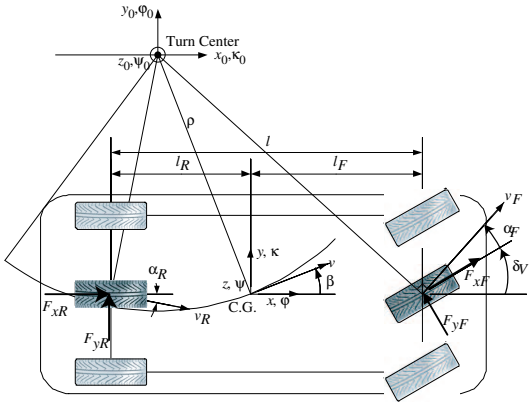

Fig. 6. Scheme for modelling the lateral vehicle behavior with the one-track model

model. For the desired model the time variant one-track model is used. A gain scheduling controller designed with the root locus design method is applied. The parameters of the controller are adjusted such that the closed loop response is stable and well damped at each operation point.

3.1 Lateral vehicle dynamics

For deriving the lateral dynamics, a coordinate system is fixed to the center of gravity (C.G.) and Newton's laws are applied. Roll, pitch, bounce, and deceleration dynamics are neglected to reduce the model to two degrees of freedom: the lateral position and yaw angle states. Further simplifications assume that each front wheel shares the same steering angle and that each wheel produces the same steering force (Fig. 6).

This leads to the one-track model of the vehicle (Börner *et al.*, 2002)

$$\begin{bmatrix} \ddot{\psi} \\ \dot{\beta} \end{bmatrix} = \begin{bmatrix} a_{11} & a_{12} \\ a_{21} & a_{22} \end{bmatrix} \begin{bmatrix} \dot{\psi} \\ \beta \end{bmatrix} + \begin{bmatrix} \frac{c_{\alpha \mathrm{F}} l_{\mathrm{F}}}{J_{\mathrm{z}} i_{\mathrm{st}}} \\ \frac{c_{\alpha \mathrm{F}}}{m\ v\ i_{\mathrm{st}}} \end{bmatrix} \delta_{\mathrm{H}}$$
$$\begin{bmatrix} \dot{\psi} \\ \ddot{y} \end{bmatrix} = \begin{bmatrix} 1 & 0 \\ c_{21} & c_{22} \end{bmatrix} \begin{bmatrix} \dot{\psi} \\ \beta \end{bmatrix} + \begin{bmatrix} 0 \\ \frac{c_{\alpha \mathrm{F}}}{m\ i_{\mathrm{st}}} \end{bmatrix} \delta_{\mathrm{H}} \tag{9}$$

with the speed dependent parameters:

$$a_{11} = -\frac{c_{\alpha \mathrm{R}} l_{\mathrm{R}}^2 + c_{\alpha \mathrm{F}} l_{\mathrm{F}}^2}{J_{\mathrm{z}} v} \qquad a_{12} = \frac{c_{\alpha \mathrm{R}} l_{\mathrm{R}} - c_{\alpha \mathrm{F}} l_{\mathrm{F}}}{J_{\mathrm{z}}}$$
$$a_{21} = \frac{c_{\alpha \mathrm{R}} l_{\mathrm{R}} - c_{\alpha \mathrm{F}} l_{\mathrm{F}}}{m\ v^2} - 1 \qquad a_{22} = -\frac{c_{\alpha \mathrm{R}} + \dot{v}\ m + c_{\alpha \mathrm{F}}}{m\ v}$$
$$c_{21} = \frac{c_{\alpha \mathrm{R}} l_{\mathrm{R}} - c_{\alpha \mathrm{F}} l_{\mathrm{F}}}{m\ v} \qquad c_{22} = -\frac{c_{\alpha \mathrm{R}} + \dot{v}\ m + c_{\alpha \mathrm{F}}}{m}$$

The symbols used are given in Table 1.

If v and $\dot{v}$ are assumed to be constant, Eq. (9) leads to

$$G_{\dot{\psi}}(s) = \frac{\dot{\psi}(s)}{\delta_{\mathrm{H}}(s)} = \frac{b_0 + b_1 s}{1 + a_1 s + a_2 s^2} \tag{10}$$

where

$$b_0 = \frac{1}{c_{\alpha \mathrm{F}} c_{\alpha \mathrm{R}} l^2 + m v^2 (l_{\mathrm{R}} c_{\alpha \mathrm{R}} - l_{\mathrm{F}} c_{\alpha \mathrm{F}})} \cdot \frac{c_{\alpha \mathrm{F}} c_{\alpha \mathrm{R}} v l}{i_{\mathrm{st}}}$$
$$b_1 = \frac{m v l_{\mathrm{F}}}{c_{\alpha \mathrm{R}} l} \cdot b_0$$
$$a_1 = \frac{J_{\mathrm{z}} v (c_{\alpha \mathrm{F}} + c_{\alpha \mathrm{R}}) + m v (l_{\mathrm{F}}^2 c_{\alpha \mathrm{F}} + l_{\mathrm{R}}^2 c_{\alpha \mathrm{R}})}{c_{\alpha \mathrm{F}} c_{\alpha \mathrm{R}} l^2 + m v^2 (l_{\mathrm{R}} c_{\alpha \mathrm{R}} - l_{\mathrm{F}} c_{\alpha \mathrm{F}})}$$
$$a_2 = \frac{J_{\mathrm{z}} m v^2}{c_{\alpha \mathrm{F}} c_{\alpha \mathrm{R}} l^2 + m v^2 (l_{\mathrm{R}} c_{\alpha \mathrm{R}} - l_{\mathrm{F}} c_{\alpha \mathrm{F}})}.$$

Table 1. Vehicle Parameters

Symbols	Description
$\dot{\psi}$	yaw rate
β	side slip angle of the vehicle body
$\alpha_{\mathrm{F,R}}$	side slip angle at the front, rear wheel
δ_{H}	steering wheel angle
i_{st}	steering system gear ratio
v	longitudinal vehicle velocity
m	vehicle mass
J_{z}	moment of inertia around the z-axis
$c_{\alpha \mathrm{F}}$	front wheel cornering stiffness
$c_{\alpha \mathrm{R}}$	rear wheel cornering stiffness
$l_{\mathrm{F}},\ l_{\mathrm{R}}$	length from front, rear axle to C.G.
ρ	radius to turn center

For the derivation of the one-track model it has been assumed that the lateral force is proportional

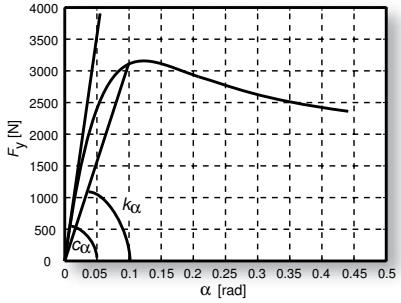

Fig. 7. Definition of the cornering stiffness c_α and the lateral stiffness k_α

to the side slip angle at the wheel (Fig. 7). However, this assumption is not valid for highly dynamic driving situations (Ammon, 1997).

3.2 Dynamic tire forces

Using the equations of the lateral forces

$$F_{\mathrm{yF}}(t) = \frac{J_{\mathrm{z}} \ddot{\psi}(t) + l_{\mathrm{R}} m \ddot{y}(t) \cos\beta + l_{\mathrm{R}} m \dot{v} \sin\beta}{(l_{\mathrm{F}} + l_{\mathrm{R}}) \cos\left(\frac{\delta_{\mathrm{H}}}{i_{\mathrm{st}}}\right)}$$
$$F_{\mathrm{yR}}(t) = \frac{-J_{\mathrm{z}} \ddot{\psi}(t) + l_{\mathrm{F}} m \ddot{y}(t) \cos\beta + l_{\mathrm{F}} m \dot{v} \sin\beta}{(l_{\mathrm{F}} + l_{\mathrm{R}})}$$

and the definition of the wheel slip angles

$$\alpha_{\mathrm{F}}(t) = -\beta(t) + \frac{\delta_{\mathrm{H}}(t)}{i_{\mathrm{st}}} - \frac{l_{\mathrm{F}} \dot{\psi}(t)}{v(t)}$$
$$\alpha_{\mathrm{R}}(t) = -\beta(t) + \frac{l_{\mathrm{R}} \dot{\psi}(t)}{v(t)}$$

a lateral stiffness coefficient k_α is defined:

$$k_{\alpha \mathrm{F}}(t) = \frac{F_{\mathrm{yF}}(t)}{\alpha_{\mathrm{F}}(t)} \qquad k_{\alpha \mathrm{R}}(t) = \frac{F_{\mathrm{yR}}(t)}{\alpha_{\mathrm{R}}(t)} \tag{11}$$

Fig. 8 depicts simulated results with Eq. (11) for a double lane change with $v = 50 \frac{\mathrm{km}}{\mathrm{h}}$. A hysteresis type curve is obtained because the dynamics in the lateral force generation are not considered.

Therefore, a dynamic spring-damper model is introduced in Fig. 9 (Ammon, 1997).

The differential equation of the model then becomes:

$$\frac{c_\alpha}{c_{\mathrm{y}} |v|} \dot{F}_y(t) + F_y(t) = c_\alpha \alpha(t)$$
$$\Rightarrow F_y(s) = \frac{c_\alpha}{Ts + 1} \alpha(s)$$
$$\text{with} \quad T = \frac{c_\alpha}{c_{\mathrm{y}} |v|}$$

Applying this model to the maneuver in Fig. 8, the reconstructed lateral stiffness $k_\alpha(t)$ leads to

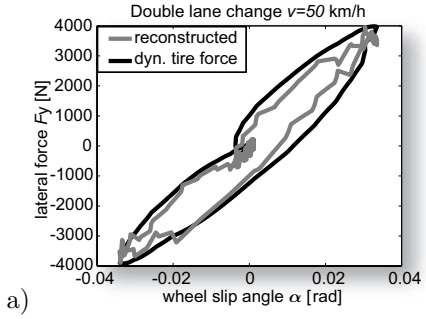

a)

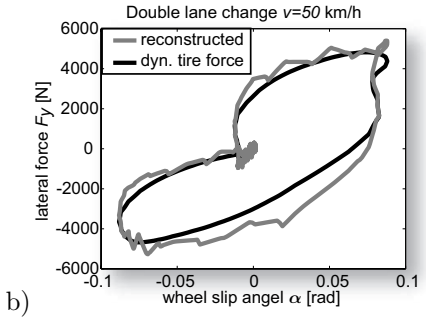

b)

Fig. 8. Lateral force F_y for a double lane change with $v = 50\frac{\mathrm{km}}{\mathrm{h}}$
a) at the rear axle
b) at the front axle

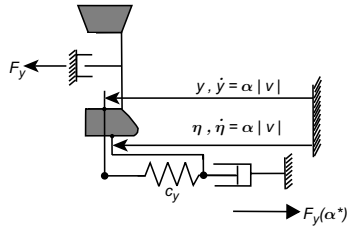

Fig. 9. Model for the dynamic tire forces

a unique curve with $c_\mathrm{y} = 100\,000\frac{\mathrm{N}}{\mathrm{m}}$ and $c_\alpha = 75\,000\frac{\mathrm{N}}{\mathrm{rad}}$. Considering different lateral stiffness c_y at the front and rear axle, the lateral force can be written as:

$$F_{\mathrm{yF,R}}(s) = \frac{c_{\alpha\mathrm{F,R}}}{T_{\mathrm{F,R}}s + 1}\alpha_{\mathrm{F,R}}(s) \tag{12}$$

with

$$T_\mathrm{F} = \frac{c_{\alpha\mathrm{F}}}{c_{\mathrm{yF}}|v|} \qquad T_\mathrm{R} = \frac{c_{\alpha\mathrm{R}}}{c_{\mathrm{yR}}|v|}$$

If this dynamic equation is applied to Eq. (10) instead of $F_\mathrm{y} = c_\alpha \cdot \alpha$, the transfer function of the one track model becomes:

$$\begin{aligned} G(s) &= \frac{\dot{\psi}(s)}{\delta_\mathrm{H}(s)} \\ &= \frac{c_0 + c_1 s + c_2 s^2}{d_0 + d_1 s + d_2 s^2 + d_3 s^3 + d_4 s^4} \end{aligned} \tag{13}$$

with:

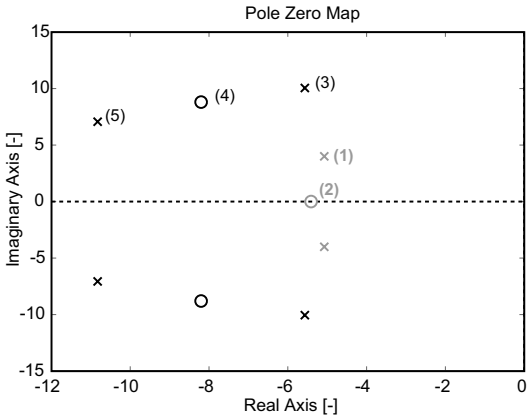

Fig. 10. Pole-zero map of the one-track model with (black) and without (grey) dynamic tire forces

$$\begin{aligned}
c_0 &= \frac{a_0 b_5 - a_4 b_0}{a_1 b_2} = \frac{c_{\alpha\mathrm{R}} \cdot c_{\alpha\mathrm{F}} \cdot (l_\mathrm{R} + l_\mathrm{F})}{J_Z \cdot T^2 \cdot m \cdot v} \\
c_1 &= \frac{-a_4 b_1}{a_1 b_2} = \frac{c_{\alpha\mathrm{F}} \cdot l_\mathrm{F}}{J_Z \cdot T^2} \\
c_2 &= \frac{-a_4 b_2}{a_1 b_2} = \frac{c_{\alpha\mathrm{F}} \cdot l_\mathrm{F}}{J_Z \cdot T} \\
d_0 &= \frac{a_3 b_0 - a_0 b_4}{a_1 b_2} \\
&= \frac{c_{\alpha\mathrm{R}} c_{\alpha\mathrm{F}} \frac{1}{v}(l_\mathrm{F}^2 + l_\mathrm{R}^2 + 2 l_\mathrm{F} l_\mathrm{R}) + mv(c_{\alpha\mathrm{R}} l_\mathrm{R} - c_{\alpha\mathrm{F}} l_\mathrm{F})}{J_Z m v T^2} \\
d_1 &= \frac{a_3 b_1 + a_2 b_0 - a_0 b_3}{a_1 b_2} \\
&= \frac{c_{\alpha\mathrm{F}}(l_\mathrm{F}^2 \frac{1}{v} + \frac{J_Z}{mv} - l_\mathrm{F} T) + c_{\alpha\mathrm{R}}(l_\mathrm{R}^2 \frac{1}{v} + \frac{J_Z}{mv} + l_\mathrm{R} T)}{J_Z T^2} \\
d_2 &= \frac{a_3 b_2 + a_2 b_1 + a_1 b_0}{a_1 b_2} \\
&= \frac{c_{\alpha\mathrm{F}}(l_\mathrm{F}^2 m + J_Z) + c_{\alpha\mathrm{R}}(l_\mathrm{R}^2 m + J_Z)}{J_Z m v T} + \frac{1}{T^2} \\
d_3 &= \frac{a_2 b_2 + a_1 b_1}{a_1 b_2} = \frac{2}{T}
\end{aligned}$$

Fig. 10 shows the distribution of poles and zeros. With Eq. (10), a new pole pair and zero pair appears. The original pole pair (1) shifts to a pole pair (3) with higher eigenfrequency.

3.3 Controller design for active steering

Based on the transfer function of the one-track-model with dynamic tire forces, a gain scheduling controller has been developed (Schmitt *et al.*, 2004*b*) (Schmitt *et al.*, 2004*a*). The controller structure is of PID-type:

$$G_c(s) = K_r + K_D s + \frac{K_I}{s} \tag{14}$$

The parameters of the gain scheduling controller was determined with a Local Linear Model ap-

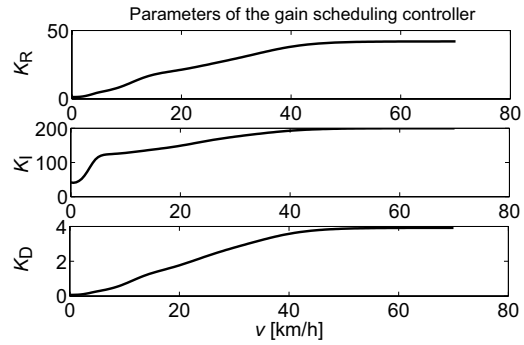

Fig. 11. Parameter of the gain scheduling controller

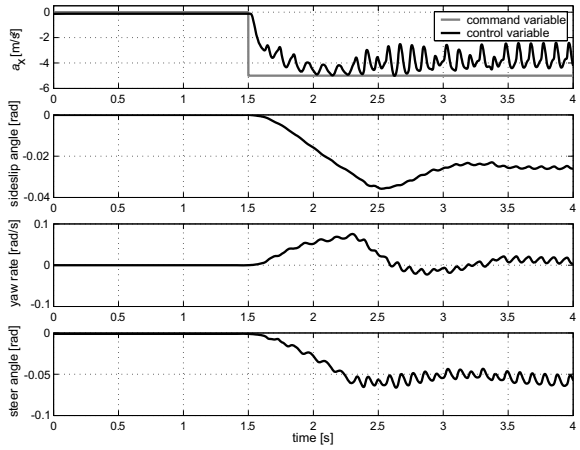

Fig. 12. Simulation results with $a_{\mathrm{x}} = -5\,\frac{m}{s^2}$ on μ-split surface using ABS and AFS

proach of the one-track model with dynamic tire forces (Schmitt *et al.*, 2004*a*).

Fig. 12 shows simulation results with the AFS stabilizing system and antilock braking. The simulated deceleration is not as high as the desired, because the friction potential is exceeded. The oscillations occur because of brake pressure pulsations caused by the antilock braking system. As can be seen, the vehicle remains stable and brakes in a straight line, despite the different μ-values. Hence, the AFS helps the driver in this critical situation.

4. SUMMARY

A model based development of drive dynamics controllers for a vehicle has been described. A braking control system has been developed and tested with simulations and test drives. To stabilize the lateral vehicle behavior, an active front steering feedback control has been added. Both systems together are able to stabilize the vehicle in critical situations. The braking control for an electrohydraulic braking system shows the expected smooth behavior on normal roads in experiments. For different road/tire friction on both sides, however, the driver has to compensate unstable behavior. Then, active front steering is of help, for generating automatically countersteering. The control design is based on a one-track model with additional dynamic tire friction. The improvement on a μ-split-road is shown using simulations.

REFERENCES

Ammon, D. (1997). *Modellbildung und Systementwicklung in der Fahrzeugdynamik*. B.G. Teubner Verlag, Stuttgart.

Breuer, B. and K. H. Bill (2003). *Bremsenhandbuch*. Vieweg Verlag. Wiesbaden.

Börner, M., L. Andreani, P. Albertos and R. Isermann (2002). Detection of lateral vehicle driving conditions based on the characteristic velocity. *Proceedings of IFAC World Congress 2002*.

Germann, S. (1997). *Modellbildung und modellgestützte Regelung der Fahrzeuglängsdynamik*. Fortschritt-Bericht Reihe 12 Nr. 309. VDI Verlag. Düsseldorf.

Halfmann, C. and H. Holzmann (2003). *Adaptive Modelle für die Kraftfahrzeugdynamik*. Springer-Verlag. Berlin.

Isermann, R., J. Schmitt, D. Fischer and M. Börner (2004). Model-based supervision and control of lateral vehicle dynamics. *3rd IFAC Symposium on Mechatronic Systems, Sydney*.

Reimpell, J. and M. Burckhardt (1991). *Fahrwerktechnik: Bremsdynamik von PKW-Bremsanlagen*. Vogel Fachbuch. Würzburg.

Robert Bosch GmbH, Ed.) (2003). *Automotive Handbook*. 5th ed.. Bentley Publishers.

Schmitt, J., M. Schorn and R. Isermann (2004*a*). Controller design for an active steering system in passenger cars based on local linear models. *Proc. of FISITA World Congress in Barcelona*.

Schmitt, J., M. Schorn and R. Isermann (2004*b*). Improving the performance of an active steering system by variation of the antiroll bar stiffness at the front and rear axle. *IFAC Symposium 'Advances in Automotive Control', April 19-23, 2004, University of Salerno, Italy*.